Available online at www.sciencedirect.com
SCIENCE DIRECT®
Materials Science and Engineering C 26 (2006) 1344 – 1350
MATERIALS SCIENCE & ENGINEERING C
www.elsevier.com/locate/msec

A biomimetic approach to the deposition of ZrO_2 films on self-assembled nanoscale templates

Guangneng Zhang [a], Jane Y. Howe [b], Dorothy W. Coffey [b], Douglas A. Blom [b], Lawrence F. Allard [b], Junghyun Cho [a,*]

[a] Department of Mechanical and Materials Engineering, P.O. Box 6000, State University of New York at Binghamton, Binghamton, NY 13902-6000, USA
[b] Metals and Ceramics Division, Oak Ridge National Lab, Oak Ridge, TN 37831, USA

Available online 3 October 2005

Abstract

Zirconium oxide thin films were deposited on a phosphonate-terminated self-assembled monolayer (SAM) on a single crystal silicon substrate by a hydrolysis of zirconium sulfate solution in acid environment at 80 °C. The ZrO_2 films consist of tetragonal ZrO_2 crystallites with a size of 5–10 nm. Surface nucleation and attraction between the SAM surface and bulk precipitates in solution can explain the film formation. In both mechanisms, the surface functionality of the SAM plays a crucial role. This deposition approach was inspired by biomineralization through controlled deposition of inorganic solids on an ordered organic matrix. Microstructures and mechanical properties of the ZrO_2 thin films were studied using scanning electron microscope (SEM), cross-sectional transmission electron microscope (TEM) and nanoindentation. Microstructures were tailored at different stages of the film growth, as well as with processing parameters and substrate surface conditions. The nanoindentation modulus and hardness of the as-deposited ZrO_2 films were much lower than those of the bulk ZrO_2. The addition of extra pressure during this process, however, restores mechanical properties of ZrO_2 films.

Keywords: Self-assembled monolayer; Zirconium oxide; TEM; Biomineralization; Biomimetic; Nanoindentation

1. Introduction

Due to excellent structural and functional properties, ceramics provide a powerful source for realization of many advanced technologies. In particular, ceramic thin films and coatings are currently being used in fuel cell electrolytes, dielectric films in semiconductor devices, thermal barrier coatings, and wear-resistant coatings [1]. In addition, ceramic films have shown a potential for protective coatings for MEMS and harsh-environment electronic devices due to their good mechanical properties and inertness [2]. Importantly, ceramic coatings and films would benefit the MEMS packaging development by relaxing the stringent requirements for the assembly [3], thereby drastically reducing the packaging cost.

Conventional ceramic processing such as powder sintering or vapor phase deposition usually requires high temperatures and sophisticated production equipment. In addition, film cracks and interfacial delamination often occurs because of shrinkage and thermal expansion mismatch. Therefore, a major challenge to produce ceramic films is to find a low-temperature synthetic route with little shrinkage, as well as to accommodate the stress development during processing.

The best example of controlling ceramic processing is often observed in nature. Since nature demonstrates how to produce complex materials and shapes with high functionality at ambient temperature, pressure and atmosphere, biomineralization has created much interest in recent years [4–7]. Frequently, biomineralization leads to the formation of highly intricate structures that are found, for instance, within bones, teeth and eggshells. According to Mann [7,8], biomineralization can be basically divided into four steps: (i) supramolecular preorganization via construction of an organized reaction environment; (ii) interfacial molecular recognition, where the preformed organic supramolecular systems provide a framework for the assembly of the inorganic phase; (iii) assembly of the mineral phase through crystal growth and termination enabling the formation of textures and shapes; (iv) formation of

* Corresponding author.
E-mail address: jcho@binghamton.edu (J. Cho).

0928-4931/$ - see front matter © 2005 Elsevier B.V. All rights reserved.
doi:10.1016/j.msec.2005.08.010

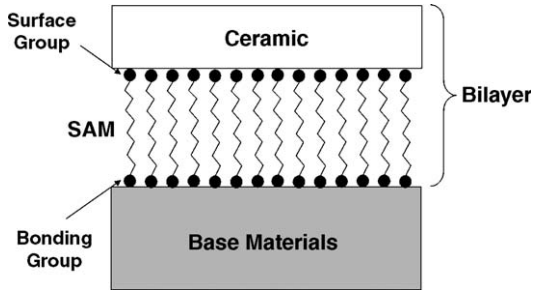

Fig. 1. Schematic illustration of deposition of ceramic thin films using self-assembled monolayer (SAM) as an organic template. Ceramic and SAM thicknesses are not in scale.

higher order architectures involving larger scale cellular activity.

Hence, an essence of biomineralization is that it is regulated by the organic component (matrix) that works as either compartments for mineralization, heterogeneous nucleation sites, substrates for specific crystallization, or scaffolds that define macroscopic shapes [8]. In this study, the principle of this biomineralization has been mimicked in the deposition of inorganic thin films using self-assembled monolayers (SAMs) as organic templates. A schematic illustration of this method is shown in Fig. 1. According to the biomimetic concept, a highly ordered array of hydrocarbon chains (SAM) is prepared by the covalent bonding of bifunctional surfactants to a substrate. The surface group of the long chain hydrocarbon molecules supports the deposition of an inorganic phase if substrates containing such a SAM are put into an appropriate solution containing suitable molecular precursors. In recent years, a variety of inorganic materials have been deposited via this approach including: TiO_2 [9–15], ZrO_2 [16–23], Y_2O_3/ZrO_2 [16], FeO(OH) [24], V_2O_5 [12], $SrTiO_3$ [25], ZnO [26], SnO_2 [27–31], $CaCO_3$ [32], Ta_2O_5 [33], La_2O_3 [34], ZnS [35], PbS [35].

Our research has focused on the synthesis of ZrO_2 thin films deposited on a SAM-coated silicon substrate via a precursor solution method at near room temperatures. A goal of this study is to generate a SAM coating suitable for ceramic deposition, on which nanocrystalline ZrO_2 films are grown. In particular, the surface of the SAM was engineered to work as an organic template. Microstructural and mechanical evolutions of the thin films were systematically assessed at various processing parameters.

2. Experiment

2.1. Deposition of SAMs

The substrates used in this study were n-type ⟨100⟩ single-crystal silicon wafers (Silicon Quest International, Santa Clara, CA). Silicon wafers were first ultrasonically cleaned with 2-propanol and acetone in sequence, rinsed with deionized water, and dried with nitrogen gas. Then the wafers were immersed in piranha solution (5 mL chilled 30% H_2O_2 solution plus 15 mL concentrated H_2SO_4). This acid cleaning activated the surface of the wafer and created an oxide layer necessary for the following SAM deposition. After cleaning, the wafers were rinsed with deionized water and dried completely with nitrogen gas.

The SAMs were then deposited on the hydrolyzed silicon wafers by immersion in a 1 vol.% diethylphosphatoethyl-triethoxysilane ($C_{12}H_{29}O_6PSi$; Gelest Inc., Morrisville, PA) in a distilled-toluene solution inside a nitrogen-filled glove bag at room temperature for 24 h. The SAMs were further hydrolyzed by immersing the wafers in 1 M HCl solution at 80 °C to obtain a suitable surface terminus ($-PO(OH)_2$) for the subsequent ZrO_2 deposition. The SAM-coated wafers were then ultrasonically cleaned with acetone and dried completely with nitrogen gas. These coatings were characterized using contact angle meter (KSV CAM100, KSV Instruments Ltd.) to check a proper surface condition before ceramic deposition.

2.2. Deposition of ZrO_2 thin films

For deposition of ZrO_2 film, reagent-grade zirconium sulfate ($Zr(SO_4)_2{\cdot}4H_2O$; Alfa Aesar, Ward Hill, MA) and hydrochloric acid (Fisher Scientific) were used without further purification. A freshly prepared 0.01 M $Zr(SO_4)_2$ + 0.4–1.0 M HCl aqueous solution was used as a precursor solution. The substrates (SAM coated silicon wafers) were immersed in the precursor solution and kept in a constant temperature oil bath set at 70–90 °C for 0.5–24 h. After desired deposition time was reached, the substrates were taken out, ultrasonically cleaned and rinsed with deionized water, and dried completely with nitrogen gas.

Hydrothermal process [36] was also used to synthesize ZrO_2 films using the same precursor solution in order to see the effect of the pressure. The substrates were kept in a 45 mL acid digestion bomb (Parr Instrument Co., Moline, IL) filled with 15 mL at 135 °C for 24 h. The pressure built in the bomb during deposition was about 5 atm. After deposition, the substrates were cleaned and dried in the same way describe above.

2.3. Characterization of ZrO_2 thin films

Microstructures of the ZrO_2 thin films were characterized by SEM and TEM. Plan-view SEM work was carried out at low accelerating voltages ($\leq$1 kV) without surface carbon coatings using field-emission gun SEM (JEOL JSM-7401F). Cross-sectional ion-milled TEM specimens were prepared and a high-resolution field-emission gun TEM (Hitachi HF-2000) was used. Mechanical properties of the ZrO_2 thin films were also studied using a nanoindentation system (TriboIndenter®, Hysitron Inc., Minneapolis, MN) with a built-in in-situ AFM imaging capability. Mechanical characterization provides a fundamental understanding of structural evolution of the ZrO_2 films with different processing conditions.

3. Results and discussions

3.1. Film formation in aqueous solution

It is required that the SAM surface be 'hydrophilic' to grow the ceramic film [23]. The contact angle measured with

a deionized water drop was ~70° for non-hydrolyzed SAMs, and became ~30° for hydrolyzed SAMs. Therefore, the SAMs were always acid hydrolyzed to have a proper surface condition. It was also found that the presence of the SAM was a necessary condition for the formation of ZrO_2 films, as reported by Agarwal et al. [16]. No significant film growth was observed on bare silicon samples under same conditions [23].

It was also necessary to condition a precursor solution in such a way that bulk precipitation was taking place while avoiding extensive precipitation. It has been reported that in the absence of bulk precipitation, films could be grown only up to 3-nm thick in a single deposition, regardless of time [16]. We found that the time needed for bulk precipitation to occur in our experiments increased with increasing HCl concentration or decreasing temperature, as shown in Fig. 2. For a 0.01 M $Zr(SO_4)_2$+0.4 M HCl precursor solution at 70 °C, bulk precipitation occurred 20 min after the solution was put into the oil bath. However, for a 0.01 M $Zr(SO_4)_2$+>0.8 M HCl precursor solution, neither bulk precipitation nor ZrO_2 film on SAM-coated substrate was observed for 24 h, as shown in Fig. 3.

It has been reported that the formation of the precipitate involves two major reactions as follows [16]. First the hydroxyl group replaces the sulfate group to form anionic species during dissolution of $Zr(SO_4)_2$:

$$2[Zr(SO_4)_2]_n + 3nH_2O \leftrightarrow n[Zr_2(OH)_3(SO_4)_4]^{3-} + 3nH^+$$

Further hydrolysis of the anions yields basic sulfate precipitates:

$$[Zr_2(OH)_3(SO_4)_4]^{3-} + 3OH^- \leftrightarrow Zr_2(OH)_6SO_4 + 3SO_4^{2-}$$

The $Zr(OH)^{3+}$ species and zirconium sulfate oligomers present in solution can undergo polymerization and condensation reactions to yield ZrO_2 [16,37]. From these reactions, it can be expected that the chemical equilibrium of the first reaction moves toward the right by decreasing the concentration of acid

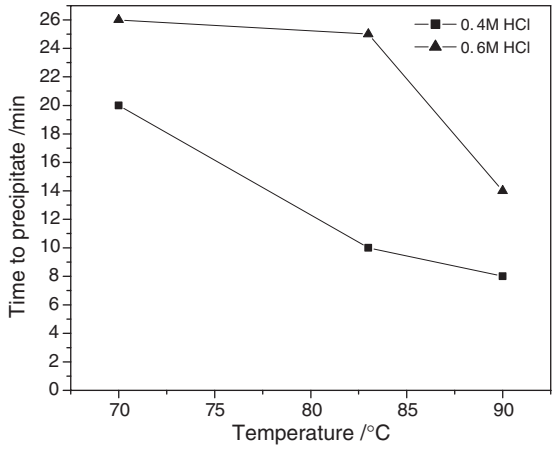

Fig. 2. Comparison of time to visible bulk precipitation for a precursor solution with different HCl concentrations at different temperatures. Bulk precipitation was not observed within 24 h for precursor solutions with HCl concentration of 0.8 M or higher.

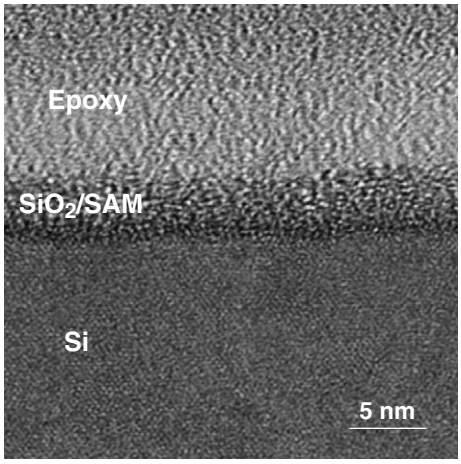

Fig. 3. Cross-sectional TEM micrograph showing absence of a ZrO_2 film on a SAM-coated Si substrate using 0.01 M $Zr(SO_4)_2$+1 M HCl precursor solution for 24 h in which bulk precipitation was inhibited by high HCl concentration.

(HCl); hence, more precipitates are yielded with decreased HCl concentration.

3.2. Nucleation and microstructure evolution

In an aqueous solution, the ceramic film formation can be achieved through two nucleation mechanisms: heterogeneous nucleation at the interface between the substrate and solution, and homogeneous nucleation by forming stable nuclei in a supersaturated solution. These mechanisms have been considered for the deposition of ZrO_2 films by immersing a SAM-coated substrate in a zirconium sulfate precursor solution. In the former mechanism, dissolved ionic species may attach to the SAM surface through an ion-by-ion growth mechanism. This is connected to directed growth of nuclei of the inorganic phase and formation of crystalline structures. Single crystal calcium carbonate has been synthesized in a similar mechanism [32,38–40]; however, little evidence of this mechanism was found for the deposition of ZrO_2 films in our study. In the latter mechanism, ZrO_2 crystals formed by homogeneous nucleation can form colloidal particles in solution and be attracted to the properly treated surface due to electrostatic interactions [10,16,41].

Fig. 4a shows ZrO_2 nanocrystallites of 5–10 nm in size formed on the functionalized surface of the SAM. In fact, our powder samples dried from the same precursor solution displayed similar sizes of the crystallites. It is, however, not clear whether they were formed via surface crystallization or homogeneous nucleation. Once these nanocrystallites are grown or formed at the surface, they attract more nanocrystallites thereby leading to the formation of isolated islands of 50–100 nm in size. These islands may further grow abnormally and connect to their neighboring islands, forming interconnected ZrO_2 islands (Fig. 4b). As deposition goes on, the island structures may grow and spread over the SAM surface, forming a continuous ZrO_2 film on the surface in several hours. At this intermediate stage of the film growth, ZrO_2 islands were prevalent, covering sparsely substrate area (Fig. 4b).

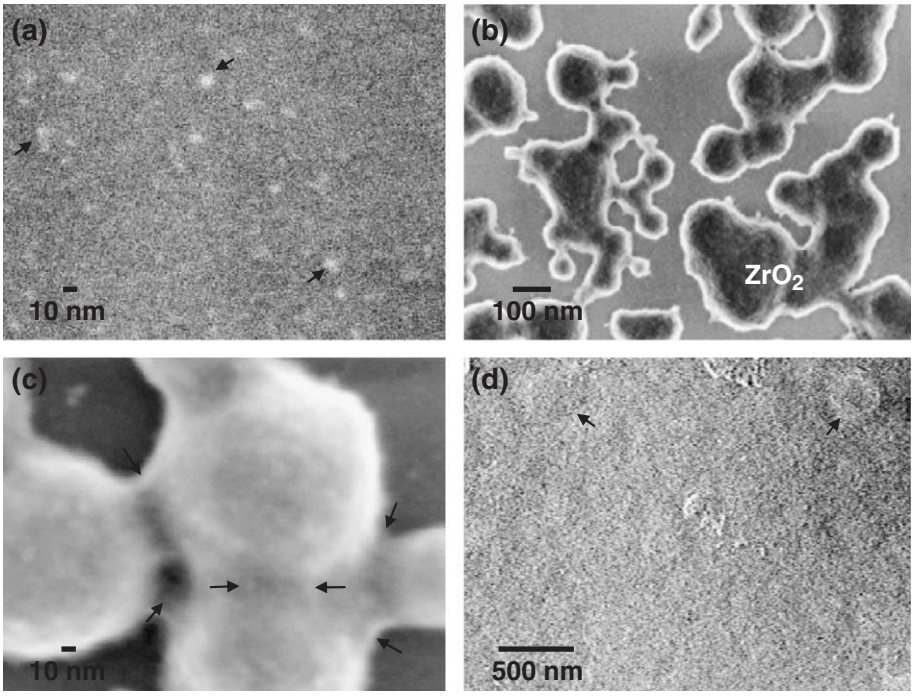

Fig. 4. Plan-view SEM images showing temporal growth of ZrO_2 films on SAM-coated silicon: (a) nanocrystallites (5–10 nm in size) at a very early stage (arrows); (b) island structures made of nanocrystals at an intermediate stage; (c) higher magnification view of the ZrO_2 islands, where arrows indicate the lateral growth of the islands; (d) continuous film formed at a final stage (arrows indicate traces of the islands).

The nucleation and growth of ZrO_2 nanocrystallites were not synchronous over all the surface. Because of non-uniformity in the microstructure development, lateral growth between the abnormally grown islands was often observed in SEM analysis as shown by arrows in Fig. 4c, suggesting that new films prefer growing on the solution-substrate interface. This phenomenon was also supported by our separate AFM analysis that the height of the ZrO_2 islands was often smaller than the island diameter by a factor of around 4 [21]. Once those islands are completely connected, a continuous, dense ZrO_2 film is obtained, wherein traces of the islands can still be seen in the films (Fig. 4d). Based on the analysis above, it is believed that the second mechanism, i.e., homogeneous nucleation, seems more responsible for the ZrO_2 film formation with our current processing settings. More systematic studies are needed to gain a fundamental understanding on the initial nanocrystal formation, and the effect of abnormal growth of the islands in certain regions.

3.3. Cross-sectional TEM characterization

Typical cross-sectional microstructures of the as-deposited ZrO_2 films prepared with 0.01 M $Zr(SO_4)_2$+0.4 M HCl precursor solutions on SAM-coated silicon wafers at 80 °C for 24 h are shown in Fig. 5. The thickness of this specific ZrO_2 film was around 50 nm. The film consists of densely packed tetragonal ZrO_2 nanocrystallites as indicated by electron diffraction (inset, Fig. 5a). The observed d-spacings from the diffraction patterns indicated d_{101}=3.017 Å, d_{002}=2.606 Å, and d_{112}=1.867 Å, which are very close to those of t-ZrO_2 structure [16]. The size of the ZrO_2 crystallites is in the range of 5–10 nm that is the same range as perceived in SEM micrographs (Fig. 4a). The orientations of the crystallites are random. The distribution of the crystallites is uniform through the thickness of the film, in contrast with that reported by Agarwal et al. [16] in that there was more crystalline phase in near-interfacial area than in far from interface area. Energy dispersive X-ray spectrometry (EDS) analyses (inset, Fig. 5b) showed a small amount of sulfur in the ZrO_2 film, suggesting the presence of remaining zirconium sulfate. The zirconium sulfate is believed to be in amorphous [10,16]. The 50-nm thick film was free of cracks and was not detached during ultrasonic vibration and rinsing with water. Fig. 5c is a magnified view of the film, in which a ZrO_2 lattice image is clearly visible.

3.4. Mechanical characterization

Nanoindentation was performed using a conical indenter on the as-deposited ZrO_2 thin film that has a thickness of 50 nm. A variety of the contact depth from 8 to 160 nm was adopted. Fig. 6 shows the reduced modulus and hardness of the ZrO_2 film/SAM/silicon structures prepared with a 0.01 M $Zr(SO_4)_2$+0.4 M HCl precursor solution on SAM-coated silicon at 80 °C for 20 h. As obviously seen from Fig. 6, both mechanical properties increase significantly at contact depths greater than 50 nm due to indentation penetrated in the silicon substrate. Therefore, the film properties was measured at contact depths shallower than 25 nm, where reduced elastic modulus is around 30 GPa and hardness is around 1 GPa. These values are much lower than those of the bulk ZrO_2 (e.g., 205 GPa [42] and 11.8 GPa [43], respectively). When contact depth is increased to more than 50 nm, reduced elastic modulus and hardness jump to around 100 GPa and 6 GPa, respectively. These values are

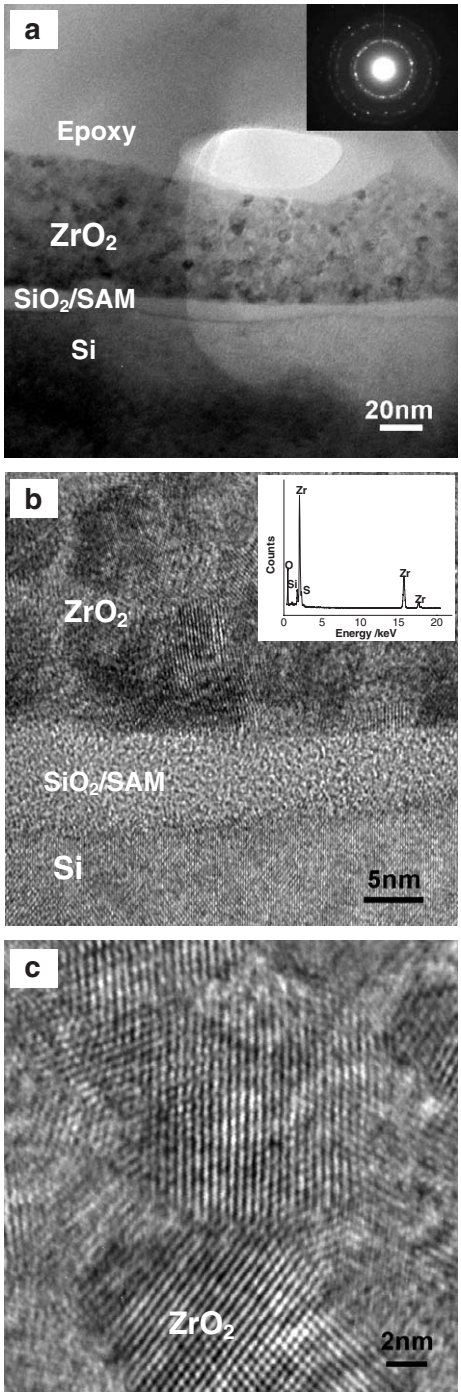

Fig. 5. (a) Cross-sectional TEM micrograph of the as-deposited ZrO_2 film on SAM-coated Si with 20 h deposition. Selected electron diffraction pattern corresponds to that of *t*-ZrO_2. (b) Higher resolution image of (a). EDS analysis shows the presence of Zr, O, S and Si. (c) ZrO_2 lattice images near the film-substrate interface.

lower than those of single-crystal silicon (170 GPa and 12 GPa, respectively) because of the presence of the compliant ZrO_2 films on top before it is indented. The low elastic modulus and hardness of the as-deposited ZrO_2 films can be attributed to the particulate structure of the film.

The mechanical properties of the ZrO_2 films prepared through a hydrothermal process were also studied (Fig. 7).

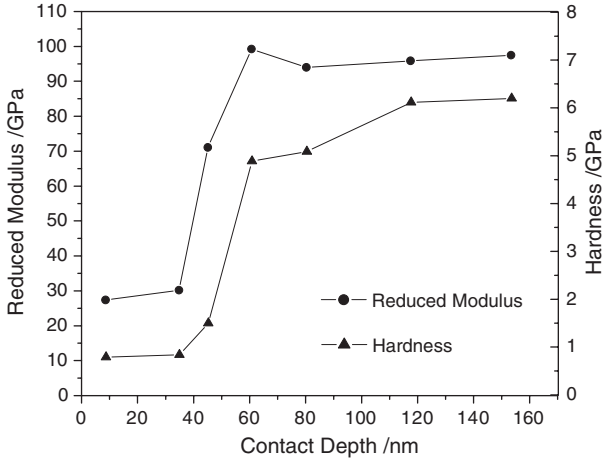

Fig. 6. Mechanical properties of the as-deposited ZrO_2 film on SAM-coated Si with 20 h deposition. Each data point represents for an average value from seven indentations. Properties with contact depths shallower than 30 nm are the true values of as-deposited ZrO_2 films.

Bare Si substrates were used in this case, as the SAM layer could be damaged in this aggressive condition. It shows higher mechanical properties of the ZrO_2 film (hardness ~9.2 GPa; modulus ~71 GPa), indicating the effect of the pressure. It seems that the pressure can offer an effective means to increasing the packing density of the films (removal of the

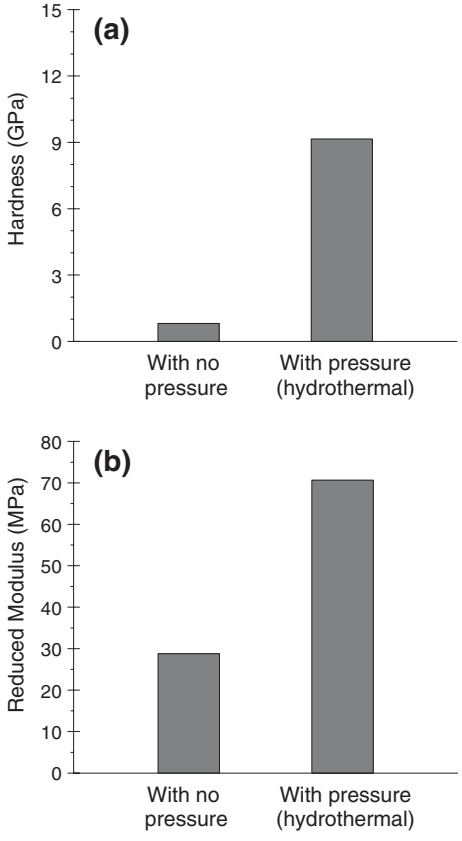

Fig. 7. Mechanical properties of the ZrO_2 films prepared with a hydrothermal process at 135 °C, ~5 atm, for 24 h, as compared to those prepared with no pressure. The data from a hydrothermal process represent for an average value from four indentations with various contact depths ranging from 65 nm to 140 nm. (a) Hardness, (b) reduced modulus.

nanoporosities), thereby providing more robust foundation on the film surface during indentation. It will be, however, challenging to incorporate this pressure process for the SAM-coated substrates.

4. Conclusion

ZrO_2 thin films were grown on phosphonate-terminated SAMs on single crystal silicon substrates by a hydrolysis of $Zr(SO_4)_2$ and HCl aqueous solution at near room temperatures. This ceramic deposition method copies the biomineralization principles and mechanisms ('biomimetic' deposition). The as-deposited ZrO_2 films consist of tetragonal ZrO_2 nanocrystals and small amount of amorphous phase (zirconium sulfate). The ZrO_2 nanocrystallites were 5–10 nm in size. Film thickness was around 50 nm for the deposition of 20 h, but it can easily vary by adjusting the level of supersaturation of the precursor solution. The principal mechanism for the nucleation and growth of the film seems to be homogeneous nucleation though the possibility of surface nucleation cannot be ruled out especially at the early stage of the film growth. One major hurdle in the microstructure development would be to avoid abnormal growth of island structures. Mechanical properties of the ZrO_2 thin film were lower than those of the bulk ZrO_2, with reduced elastic modulus of 30 GPa and hardness of 1 GPa. The presence of extra pressure can significantly increase mechanical properties by adjusting the packing density.

Acknowledgments

This work was co-sponsored by the Semiconductor Research Corporation (SRC) under contract number SRC 2003-TJ-1068 (monitored by Dr. H. Hosack) and by the Microelectronics Design Center (MDC) under contract number C000063. The TEM research was sponsored by the Assistant Secretary for Energy Efficiency and Renewal Energy, Office of FreedomCAR and Vehicle Technologies, as part of the High Temperature Materials Laboratory User Program, Oak Ridge National Laboratory, managed by UT-Battelle, LLC, for the U.S. Department of Energy under contract number DE-AC05-00OR22725. GZ and JC would also like to thank Mr. T. Kanazawa at JEOL USA, Inc. for helping with high-resolution SEM work.

References

[1] D.I. Pantelis, P. Psyllaki, N. Alexopoulos, Wear 237 (2000) 197.
[2] N. Rajan, C.A. Zorman, M. Mehregany, R. DeAnna, R. Harvey, Thin Solid Films 315 (1998) 170.
[3] N. Maluf, An Introduction to Microelectromechanical Systems, Artech House, Inc., Norwood, MA, 2000.
[4] E. Baeuerlein, Biomineralization: From Biology to Biotechnology and Medical Application, Wiley-VCH, Weinheim, 2000.
[5] H.A. Lowenstam, S. Weiner, On Biomineralization, Oxford University Press, Inc., New York, 1989.
[6] S. Mann, Journal of the Chemical Society. Dalton Transactions (1993) 1.
[7] S. Mann, Biomineralization: Principles and Concepts in Bioinorganic Materials Chemistry, Oxford University Press, Inc., New York, 2001.
[8] S. Mann, Biomimetic Materials Chemistry, VCH, New York, 1996.
[9] R.J. Collins, H. Shin, M.R. DeGuire, A.H. Heuer, C.N. Sukenik, Applied Physics Letters 69 (1996) 860.
[10] H. Shin, M. Agarwal, M.R. De Guire, A.H. Heuer, Proceedings of the 1996 Symposium on Synergistic Synthesis of Inorganic Materials, Mar 17–22 1996, Acta Materialia, vol. 46, 1998, p. 801.
[11] Y. Masuda, D. Wang, T. Yonezawa, K. Koumoto, Site-Selective Deposition of TiO_2 Thin Films Using Self-Assembled Monolayers and their Dielectric Properties, Asian Ceramic Science for Electronics II Proceedings of the 2nd Asian Meeting of Electroceramics, Oct 1 2001, vol 228–229, Trans Tech Publications Ltd, Kawasaki, Japan, 2002, p. 125.
[12] T.P. Niesen, J. Wolff, J. Bill, M.R. De Guire, F. Aldinger, Proceedings of the 1999 MRS Spring Meeting-Symposium DD, 'Organic/Inorganic Hybrid Materials', Apr 5–Apr 9 1999, vol. 576, 1999, p. 197.
[13] H. Shin, R.J. Collins, M.R. De Guire, A.H. Heuer, C.N. Sukenik, Journal of Materials Research 10 (1995) 699.
[14] H. Shin, R.J. Collins, M.R. De Guire, A.H. Heuer, C.N. Sukenik, Journal of Materials Research 10 (1995) 692.
[15] Y. Masuda, T. Sugiyama, W.S. Seo, K. Koumoto, Chemistry of Materials 15 (2003) 2469.
[16] M. Agarwal, M.R. De Guire, A.H. Heuer, Journal of the American Ceramic Society 80 (1997) 2967.
[17] A.D. Polli, T. Wagner, A. Fischer, G. Weinberg, F.C. Jentoft, R. Schloegl, M. Ruehle, Thin Solid Films 379 (2000) 122.
[18] J. Wang, S. Yang, X. Liu, S. Ren, F. Guan, M. Chen, Applied Surface Science 221 (2004) 272.
[19] V.V. Roddatis, D.S. Su, E. Beckmann, F.C. Jentoft, U. Braun, J. Krohnert, R. Schlogl, Surface and Coatings Technology 151–152 (2002) 63.
[20] Y. Gao, Y. Masuda, T. Yonezawa, K. Koumoto, Nippon Seramikkusu Kyokai Gakujutsu Ronbunshi/Journal of the Ceramic Society of Japan 110 (2002) 379.
[21] Q. Yang, G. Zhang, K. Chitre, J. Cho, Mechanical Behavior of Ceramic/SAM Bilayer Coatings, Proceedings of the 2004 MRS Fall Meeting-Symposium Y, 'Mechanical Properties of Bioinspired and Biological Materials', Nov 29–Dec 3 2004, vol. 844, Materials Research Society, Warrendale, PA, 2005, p. 333.
[22] T. O. Salami, Q. Yang, K. Chitre, S. Zarembo, J. Cho, S. R. J. Oliver, Journal of Electronic Materials 34 (2005) 534.
[23] K. Chitre, Q. Yang, T. O. Salami, S.R. Oliver, J. Cho, Journal of Electronic Materials 34 (2005) 528.
[24] B.J. Tarasevich, P.C. Rieke, J. Liu, Chemistry of Materials 8 (1996) 292.
[25] Y. Gao, Y. Masuda, K. Koumoto, Chemistry of Materials 15 (2003) 2399.
[26] M.R. DeGuire, T.P. Niesen, S. Supothina, J. Wolff, J. Bill, C.N. Sukenik, F. Aldinger, A.H. Heuer, M. Ruehle, Zeitschrift fuer Metallkunde/Materials Research and Advanced Techniques 89 (1998) 758.
[27] S. Supothina, M.R. De Guire, Thin Solid Films 371 (2000) 1.
[28] S. Supothina, Gas Sensing Properties of Nanocrystalline SnO_2 Thin Films Prepared by Liquid Flow Deposition, Proceedings of the Ninth International Meeting on Chemical Engineering, Jul 7–10 2003, vol. 93, Elsevier, Boston, MA, United States, 2003, p. 526.
[29] U. Sampathkumaran, S. Supothina, R. Wang, M.R. De Guire, Materials Research Society Symposium-Proceedings: Mineralization in Natural and Synthetic Biomaterials, Nov 29–Dec 1 1999, vol. 599, 2000, p. 177.
[30] S. Supothina, M.R. De Guire, T.P. Niesen, J. Bill, F. Aldinger, A.H. Heuer, Proceedings of the 1999 MRS Spring Meeting-Symposium DD, 'Organic/Inorganic Hybrid Materials', Apr 5–Apr 9 1999, vol. 576, 1999, p. 203.
[31] N. Shirahata, Y. Masuda, T. Yonezawa, K. Koumoto, Langmuir 18 (2002) 10379.
[32] J. Aizenberg, A.J. Black, G.M. Whitesides, Journal of the American Chemical Society 121 (1999) 4500.
[33] Y. Masuda, S. Wakamatsu, K. Koumoto, Journal of the European Ceramic Society 24 (2004) 301.
[34] Y. Gao, Y. Masuda, K. Koumoto, Journal of Colloid and Interface Science 274 (2004) 392.
[35] F.C. Meldrum, J. Flath, W. Knoll, Thin Solid Films 348 (1999) 188.
[36] R.P.J. Denkewicz, K.S. TenHuisen, J.H. Adair, Journal of Materials Research 5 (1990) 2698.

[37] B. Aiken, W.P. Hsu, E. Matijevic, Journal of Materials Science 25 (1990) 1886.
[38] J. Aizenberg, A.J. Black, G.M. Whitesides, Nature 398 (1999) 495.
[39] J. Aizenberg, Advanced Materials 16 (2004) 1295.
[40] J. Aizenberg, D.A. Muller, J.L. Grazul, D.R. Hamann, Science 299 (2003) 1205.
[41] J. Bill, R.C. Hoffmann, T.M. Fuchs, F. Aldinger, Zeitschrift fuer Metallkunde/Materials Research and Advanced Techniques 93 (2002) 478.
[42] J.F. Shackelford, W. Alexander, CRC Materials science and Engineering Handbook, CRC Press, Boca Raton, FL, 2001, p. 766.
[43] J.F. Shackelford, W. Alexander, CRC Materials Science and Engineering Handbook, CRC Press, Boca Raton, FL, 2001, p. 724.